Bioorganic & Medicinal Chemistry 20 (2012) 86–95

Contents lists available at SciVerse ScienceDirect

Bioorganic & Medicinal Chemistry

journal homepage: www.elsevier.com/locate/bmc

Investigation of substituted 6-aminohexanoates as skin penetration enhancers

Katerina Brychtova [a], Lenka Dvorakova [a], Radka Opatrilova [a], Ivan Raich [b], Sandra Kacerova [b], Lukas Placek [c], Danuta S. Kalinowski [d,*], Des R. Richardson [d,*], Josef Jampilek [a,*]

[a] Department of Chemical Drugs, Faculty of Pharmacy, University of Veterinary and Pharmaceutical Sciences Brno, Palackeho 1/3, 612 42 Brno, Czech Republic
[b] Department of Chemistry of Natural Compounds, Faculty of Food and Biochemical Technology, Institute of Chemical Technology, Technicka 5, 166 28 Prague 6, Czech Republic
[c] Pragolab s.r.o., Nad Krocinkou 55/285, 190 00 Prague 9, Czech Republic
[d] Department of Pathology and Bosch Institute, University of Sydney, Sydney, New South Wales 2006, Australia

ARTICLE INFO

Article history:
Received 11 August 2011
Revised 13 November 2011
Accepted 16 November 2011
Available online 28 November 2011

Keywords:
ω-Lactam derivatives
6-Aminohexanoic acid derivatives
Lipophilicity
Ab initio calculations
Molecular dynamic simulations
3D structures
Transdermal penetration enhancers
Anti-proliferative activity

ABSTRACT

Skin penetration enhancers are compounds used to facilitate the transdermal delivery of drugs that are otherwise not sufficiently permeable. Through a synthetic route implementing two series of esters, we generated transdermal penetration enhancers by a multi-step reaction with substituted 6-aminohexanoic acid. We present the synthesis of all newly prepared compounds here with structural confirmation accomplished by ^{1}H NMR, ^{13}C NMR, IR and mass spectroscopy (MS). The lipophilicity ($\log k$) of all compounds was determined via RP-HPLC and their hydrophobicity ($\log P$/C$\log P$) was also calculated using two commercially available programs. Ab initio calculations of geometry and molecular dynamic simulations were employed to investigate the 3-dimensional structures of selected compounds. The transdermal penetration-enhancing activity of all the synthesized esters were examined in vitro and demonstrated higher enhancement ratios than oleic acid. Compounds **2e** (C_{10} ester chain) and **2f** (C_{11} ester chain) exhibited the highest enhancement ratios. It can be concluded that the series non-substituted at the $C_{(2)}$ position by a ω-lactam ring showed significantly higher activity than those with azepan-2-one. None of the prepared compounds penetrated through the skin. All of the investigated agents demonstrated minimal anti-proliferative activity using the SK-N-MC neuroepithelioma cell line (IC_{50} >6.25 μM), suggesting these analogs would have a low cytotoxic profile when administered in vivo as chemical penetration enhancers. The correlation between the chemical structure of the studied compounds and their lipophilicity is discussed in regards to transdermal penetration-enhancing activity.

1. Introduction

Transdermal delivery systems remain an alternative administration route to conventional forms of pharmaceutical administration. However, application of this therapeutic system remains problematic due to insufficient or lack of penetration by active pharmaceutical agents through the skin.[1–3] The stratum corneum, the outermost layer of skin, forms a barrier against exogenous substances, such as pharmaceutical drugs. This barrier quality is attributed to the multi-layered structure of the stratum corneum, where terminally differentiated keratin-rich epidermal cells (keratinocytes) are embedded in a lipid-rich intercellular matrix. In order to overcome the barrier properties of skin, either physical or chemical (using penetration enhancers) techniques or biochemical methods have been implemented.[1–3]

Transdermal penetration enhancers, interact with skin components to allow the entry of drugs from a topical application into the circulation. A vast number of compounds from various chemical classes have been examined as transdermal penetration enhancers and numerous sites and modes of action have been identified.[3–6] Despite considerable research, chemical penetration enhancers have not been widely applied in transdermal systems to date.

Chemical penetration enhancers are compounds that partition into and can directly interact with components of the stratum corneum when included in a transdermal formulation. This results in a reduction of the resistance of the skin to drug diffusion. Although the exact mechanism of action of enhancers has not been elucidated, several possible hypotheses exist regarding their activity and it is possible that they may act via multiple effects. Collectively, chemical penetration enhancers may act by: (i) promoting partitioning (by influencing the nature of the stratum corneum, resulting in an increase in the penetrant concentration gradient and, hence, increasing the flux, that is, elevating the drug concentration in the skin); (ii) interacting with the intercellular lipid matrix (particularly ceramides); or by (iii) interacting with protein

* Corresponding authors. Tel.: +420541562925 (J.J.); tel.:+61290366548 (D.R.R.); tel.:+61290366547 (D.S.K.).
E-mail addresses: danuta.kalinowski@sydney.edu.au (D.S. Kalinowski), d.richardson@med.usyd.edu.au (D.R. Richardson), josef.jampilek@gmail.com, jampilekj@vfu.cz (J. Jampilek).

0968-0896/$ - see front matter © 2011 Elsevier Ltd. All rights reserved.
doi:10.1016/j.bmc.2011.11.033

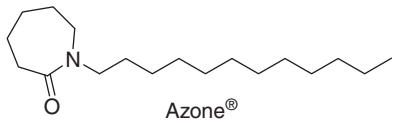

Figure 1. Dodecylazacycloheptan-2-one or *N*-dodecylcaprolactam (Azone®).

structures (altering the conformation of proteins in desmosomes or keratin in keratinocytes).[3]

One of the most studied chemical penetration enhancers, dodecylazacycloheptan-2-one (Azone®; see Fig. 1), contains a lipid alkyl chain and a large polar head group that are thought to be vital for activity[3,4] and its possible mechanism of action has been described.[3,4,7,8] The chemical structure of Azone® is derived from decylmethylsulfoxide and pyrrolidone, both of which are potential penetration enhancers.[9] Interestingly, many Azone®-related analogs (including those containing modifications in the lipophilic chain and/or heterocyclic moiety) have been synthesized and examined as chemical penetration enhancers.[3] Importantly, 6-aminohexanoic acid esters have been investigated as acyclic Azone® analogs,[3] while the piperidin-2-one, pyrrolidin-2,5-dione and morpholine moieties are also chemical fragments of chemical penetration enhancers. The compounds described in this investigation are novel and represent a combination of drug fragments which show high efficiency as transdermal penetration enhancers.[3,10–12]

Herein, the multi-step synthesis of a new series of chemical penetration enhancers is reported which includes seven alkyl-6-(2,5-dioxopyrrolidin-1-yl)hexanoates and seven alkyl-6-(2,5-dioxopyrrolidin-1-yl)-2-(2-oxoazepan-1-yl)hexanoates containing C_6–C_{12} linear alkyl ester chains. The well-known physico-chemical descriptor of lipophilicity, log*P*, is largely employed during quantitative structure–activity relationship analysis. In a number of studies examining penetration enhancement, the relationship between lipophilicity and their potency of penetration enhancement was investigated.[13–17] Thus, in the current investigation we examined both the calculated lipophilicity (log*P*/*C*log*P*) and the experimental lipophilicity log*k* data[18] of all compounds to determine if this factor plays a role in their penetration enhancement potency. In addition, as physico-chemical properties, including planarity, can influence transdermal penetration, we have investigated the geometry of four selected compounds through molecular dynamic simulations and ab initio calculations and we present their predicted 3-dimensional structures. To evaluate the transdermal penetration-enhancing activity of all synthesized esters in vitro, a Franz cell was implemented.[19] Further, all the discussed compounds were evaluated for their anti-proliferative activity against cells in culture to assess any detrimental cytotoxic activity.[20] The structure–activity relationships derived from these analyses are discussed in terms of designing effective chemical penetration enhancers.

2. Results and discussion

2.1. Chemistry

In our multi-step synthetic scheme, 6-aminohexanoic acid and succinic anhydride were used as starting reagents, yielding 6-(2,5-dioxopyrrolidin-1-yl)hexanoic acid (**1**) (Scheme 1). The reaction of acid **1**, *N*,*N*′-dicyclohexylcarbodiimide (DCC), an appropriate primary alcohol and a catalytic amount of 4-(dimethylamino)pyridine (DMAP) yielded the desired alkyl-6-(2,5-dioxopyrrolidin-1-yl)hexanoates, **2a**–**g**.

As reported previously,[23] using an optimised Schwenk and Papa procedure,[21,22] **1** gave ethyl-2-bromo-6-(2,5-dioxopyrrolidin-1-yl)hexanoate (**3**) through a one pot synthesis. Ethyl-6-(2,5-dioxopyrrolidin-1-yl)-2-(2-oxoazepan-1-yl)hexanoate (**4**) was synthesized from the α-bromocarboxylic compound, **3**, and azepan-2-one using the heterogeneous catalyst, powdered copper(I) oxide.[23,24]

The desired alkyl-6-(2,5-dioxopyrrolidin-1-yl)-2-(2-oxoazepan-1-yl)hexanoates (**5a–g**) were prepared by the base-catalyzed transesterification[25] of **4** in the presence of an excess of the corresponding primary unbranched alcohol (Scheme 1).

2.2. Lipophilicity of the prepared compounds

The calculated hydrophobicity (log*P*/*C*log*P* values) of compounds **2a**–**g** and **5a**–**g** were obtained using two commercial programs (ChemOffice Ultra 10.0[26] and ACD/LogP DB[27]). Addition-

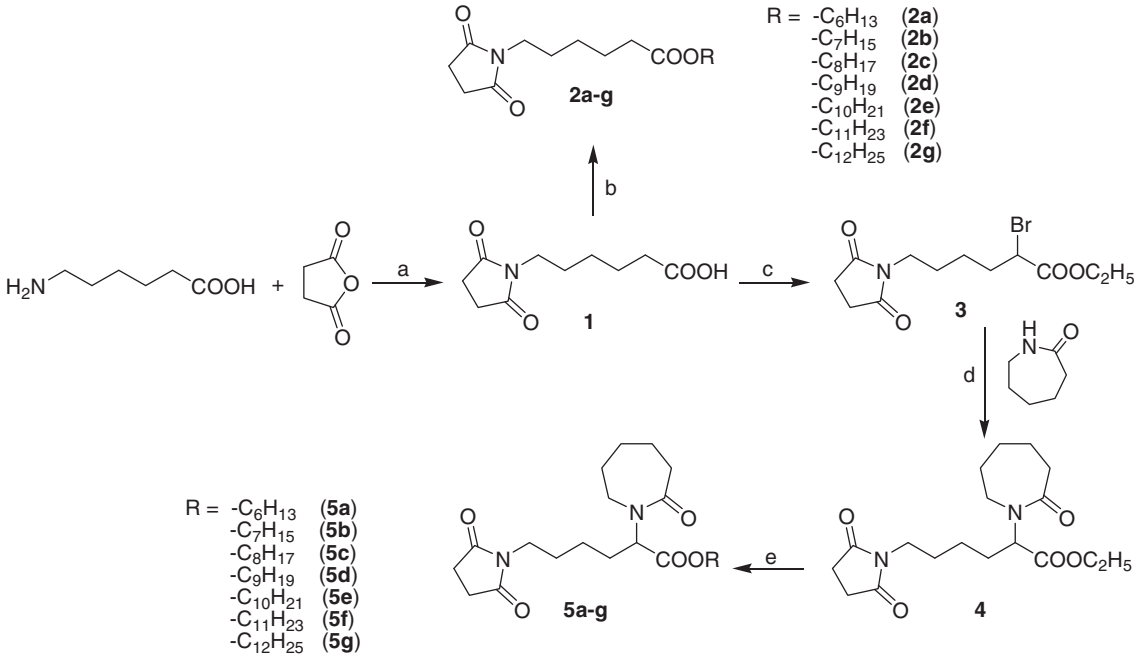

Scheme 1. Synthesis of target compounds **2a**–**g** and **5a**–**g**. Reagents: (a) Acetone; (b) DCC, DMAP, CH_2Cl_2; (c) one pot synthesis: $SOCl_2$, Br_2, EtOH; (d) NaH, DMF, Cu_2O; (e) Na, R-OH.

Table 1
Comparison of calculated lipophilicities (log*P*/Clog*P*) with determined log*k* values

Compd	log*k*	Log*P*/Clog*P* (ChemOffice)	log*P* (ACD/LogP DB)	ER	SK-N-MC IC_{50} (μM)
2a	−0.0201	2.21/2.774	2.72 ± 0.37	2.71 ± 0.20	>6.25
2b	0.1500	2.63/3.303	3.25 ± 0.37	2.64 ± 0.18	>6.25
2c	0.3239	3.05/3.832	3.79 ± 0.37	2.55 ± 0.19	>6.25
2d	0.4901	3.47/4.361	4.32 ± 0.38	3.14 ± 0.22	>6.25
2e	0.6548	3.88/4.890	4.85 ± 0.38	3.54 ± 0.16	>6.25
2f	0.8368	4.30/5.419	5.38 ± 0.38	3.51 ± 0.24	>6.25
2g	1.0091	4.72/5.948	5.91 ± 0.38	2.93 ± 0.12	>6.25
5a	−0.0764	2.19/3.431	3.19 ± 0.57	1.93 ± 0.14	>6.25
5b	0.0658	2.60/3.960	3.72 ± 0.57	—[b]	>6.25
5c	0.2462	3.02/4.489	4.25 ± 0.57	2.24 ± 0.18	>6.25
5d	0.4095	3.44/5.018	4.79 ± 0.57	1.87 ± 0.19	>6.25
5e	0.6158	3.86/5.547	5.32 ± 0.57	—[b]	>6.25
5f	0.7462	4.27/6.076	5.85 ± 0.57	1.81 ± 0.21	>6.25
5g	0.9081	4.69/6.605	6.38 ± 0.57	2.48 ± 0.19	>6.25
OA	—[a]	6.29/7.7860	7.42 ± 0.20	1.13 ± 0.18	—
Dp44mT	—	—	—	—	0.01 ± 0.01
DFO	—	—	—	—	17.07 ± 3.77

Enhancement ratios (ERs) of the prepared compounds, **2a–g** and **5a–g**, and oleic acid (OA) and in vitro anti-proliferative activity of the studied compounds using SK-N-MC neuroepithelioma cells. Enhancement ratio data are expressed as mean ± SD (n = 3 experiments) and anti-proliferative activity of the compounds are expressed as mean ± SD (n = 3 experiments).

[a] Log*k* value was not determined.

[b] Not tested due to low yield.

ally, we measured their experimental hydrophobicities by RP-HPLC to determine their capacity factors (k) with the subsequent calculation of their log*k* values. This involved the measurement of compound retention times using isocratic conditions with various amounts of an organic solvent (methanol) in the mobile phase. The capacity factor, k, was calculated using a non-polar C_{18} stationary RP column and the corresponding log*k* value (Table 1) was used as a lipophilicity index converted to the log*P* scale.[18]

Contrary to our experimental log*k* data and the calculated ChemOffice results, the data calculated by the ACD/LogP DB program showed that the non-2-substituted series, **2a–g**, was more hydrophilic than the azepan-2-one series, **5a–g**. The lower lipophilicity of the azepan-2-one series, **5a–g**, as determined by experimental log*k* data and the calculated ChemOffice results may be due to intra-molecular interactions between the lactam carbonyl moiety and other sterically close carbonyl groups.

Both **2a** and **5a** showed the highest hydrophilicity, whereas the analogues with the longest alkyl chains, dodecyl-6-(2,5-dioxopyrrolidin-1-yl)hexanoate (**2g**) and dodecyl-6-(2,5-dioxopyrrolidin-1-yl)-2-(2-oxoazepan-1-yl)hexanoate (**5g**), were the most lipophilic within each series. As expected, the calculated log*P*/Clog*P* data and experimental log*k* values corresponded to the expected trend in lipophilicity within each series of evaluated compounds (hexyl < heptyl < nonyl < decyl < undecyl < dodecyl derivatives), with this dependence being approximately linear.

2.3. In vitro anti-proliferative activity

Many iron chelating agents contain carbonyl-containing moieties that are potential donor atoms and show anti-proliferative effects due to the vital role of iron in cell growth and DNA synthesis.[28] Considering their structures (Scheme 1), it was possible that some of the novel transdermal penetration enhancers could weakly bind iron or, more likely, have anti-proliferative activity due to other mechanisms of action. Since these chemical penetration enhancers will be applied topically, side effects due to cytotoxicity are important to assess in terms of choosing lead compounds with greatest activity, but lowest toxicity. We chose the SK-N-MC neuroepithelioma cell line for these studies (Table 1) as they have been extensively used in our laboratory for assessing the anti-proliferative efficacy of iron chelators.[29–31] In addition, these novel compounds were assessed in comparison to two positive controls, namely desferrioxamine (DFO), a clinically used iron chelator, and di-2-pyridylketone 4,4-dimethyl-3-thiosemicarbazone (Dp44mT), a ligand with potent anti-tumour activity.[29–31] Both DFO and Dp44mT have been extensively examined in our laboratory in previous studies and their activity is well described.[28–31]

All of the currently studied alkyl esters, **2a–g** and **5a–g**, showed low anti-proliferative activity, all having IC_{50} values >6.25 μM (Table 1). In agreement with our previous studies,[29,31] the cytotoxic chelator, Dp44mT (IC_{50}: 0.01 μM), was effective at inhibiting the proliferation of the SK-N-MC cell line, while the standard iron chelator, DFO (IC_{50}: 17.07 μM), had poor anti-proliferative activity (Table 1). The poor anti-proliferative activity of our alkyl ester, **2a–g** and **5a–g**, suggests that these compounds will have limited cytotoxic effects when used as chemical penetration enhancers in vivo, supporting their pharmaceutical development.

2.4. Computational studies

Importantly, both the chemical structure and the exact 3D geometry of the novel chemical penetration enhancers are crucial factors that influence their physico-chemical properties and determine their penetration-enhancing activity.[3,32–34] Additionally, structural descriptors including molecular dimensions, volume and surface, dipole moment etc., are often used for *in silico* screening and the design of new chemical penetration enhancers.[3,33] Azone®-like enhancers may act via several possible mechanisms, one being the intercalation between ceramides in the stratum corneum, in turn disrupting ceramide-ceramide *H*-bonds and binding firmly to ceramide molecules to form a 'channel' in the stratum corneum.[3,7] Significantly, as intercalation potency is dependent on the planar conformation of chemical penetration enhancers, examining the 3D structures of the chemical penetration enhancers in the current study is of importance. Considering these factors, computational studies were conducted with three main objectives in mind: (i) to assess the preferred conformations of our novel chemical penetration enhancers; (ii) to assess their conformational flexibility; and (iii) to verify how these structures fit established models of penetration enhancers. Furthermore, the geometric conformations of the chemical penetration enhancers are discussed in relation to their measured in vitro enhancement activity.

Of both series of compounds synthesized in this work, the shortest and the longest alkyl derivatives, that is, compounds **2a**,

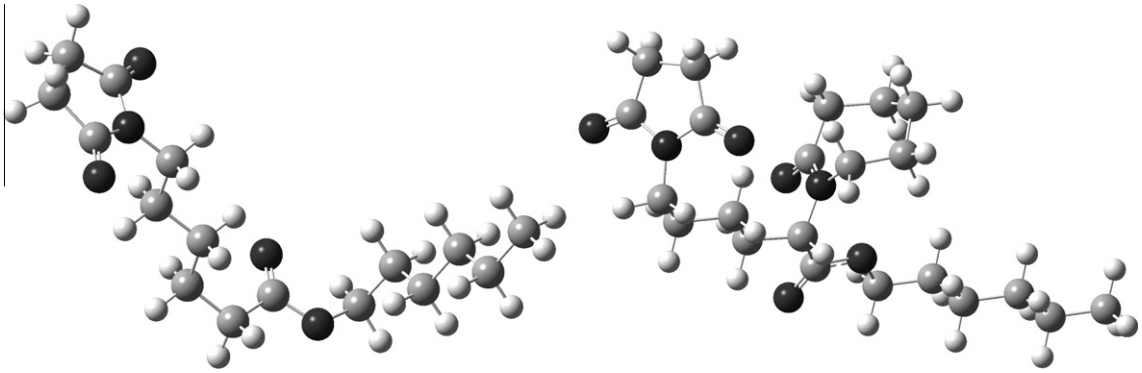

Figure 2. Global geometry optima for the *S*-enantiomers of hexyl-6-(2,5-dioxopyrrolidin-1-yl)hexanoate (**2a**) and hexyl-6-(2,5-dioxopyrrolidin-1-yl)-2-(2-oxoazepan-1-yl)hexanoate (**5a**).

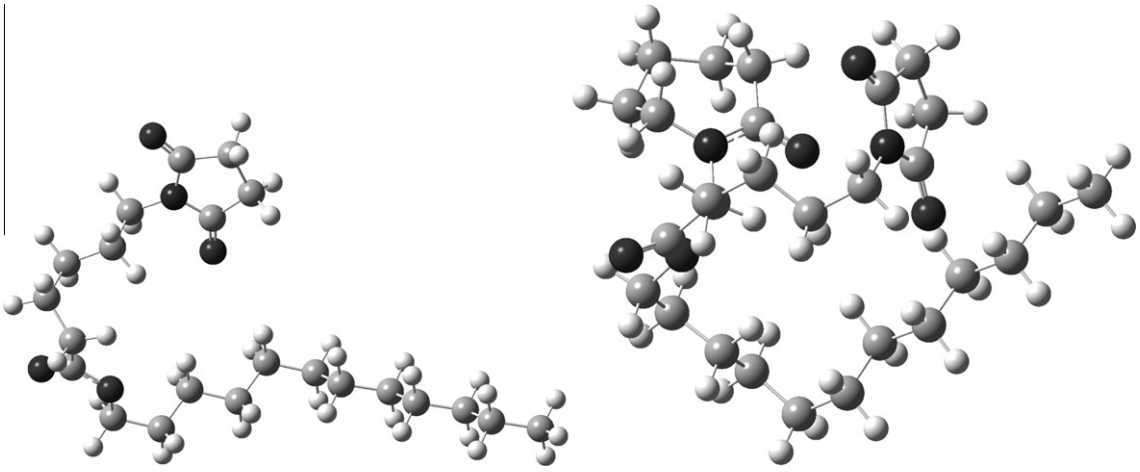

Figure 3. 3D structure of the *S*-enantiomer of dodecyl-6-(2,5-dioxopyrrolidin-1-yl)hexanoate (**2g**) and dodecyl-6-(2,5-dioxopyrrolidin-1-yl)-2-(2-oxoazepan-1-yl)hexanoate (**5g**).

5a and **2g**, **5g**, respectively, were chosen for computational studies. Due to the size and flexibility of the molecules, a combination of quantum mechanics and molecular mechanics methods was used during geometry optimizations, as described previously.[12] Low energy conformers were first searched using the conformational search utility in HyperChem with the MM+ forcefield.[35] About 35,000 conformations were scanned for each compound. Conformations with relative energy <2 kcal/mol were taken for a subsequent optimization step performed in water at the HF/4–31G level in Gaussian 09W.[36] The final optimization step was accomplished using the Becke three parameter and Perdew and Wang's 1991 hybrid functional B3PW91[37,38] and 6–31G(d,p)[39,40] basis set. The structures only poorly converged to minima and the convergence was significantly improved using the ultrafine integration grid.[41] Global energy minima found for all compounds are given in Figures 2 and 3.

While the hexyl chain adopts a zig–zag conformation in both derivatives, **2a** and **5a** (Fig. 2), the dodecyl chain contains one (**5g**) or two (**2g**) gauche orientations between anti-periplanar regions in the alkyl ester chain (Fig. 3). Similarly, alkyl chains of hexanoate residues adopt a zig–zag conformation in hexyl esters **2a** and **5a**, or have one (**2g**) or two (**5g**) gauche orientations in the case of dodecyl esters (Figs. 2 and 3, respectively). The azepan ring adopts a chair conformation in both **5a** and **5g** (Figs. 2 and 3). Molecular volumes and solvent accessible surfaces (probe radius 1.4 Å) are given in Table 2.

Table 2
Molecular volumes and solvent accessible surfaces

Compd	Mol volume (Å^3)	Mol surface (Å^2)
2a	996.85	609.39
2g	1293.94	758.20
5a	1246.21	707.30
5g	1493.72	765.35

While ab initio calculations provide a good static picture of the low energy conformers, molecular dynamics simulations were used to assess conformational flexibility and behaviour with a better representation of the solvent media. Molecular dynamics provides a simulation of physical movements of atoms and molecules. As noted previously,[11,12] the solvent is usually quite poorly represented by ab initio calculations. For the above calculations at the ab initio level, the solvent used during our in vitro experiments (propylene glycol/water 1:1 v/v) was simplified so that propylene glycol molecules were omitted and water molecules were replaced by a dielectric continuum using the conductor-like polarizable continuum model.

Using the periodic box[12] filled with a mixture of propylene glycol/water (0.5:0.5 v/v), a series of molecular dynamics assessments for compounds **2a**, **2g, 5a** and **5g** were initiated from the lowest energy conformations. Preparation of the periodic box (a mixture of *R*/*S* enantiomers of propylene glycol and water) with the solute was described previously.[12] Mean values of selected torsions

Table 3
Torsion angles in (°) of compounds **2a**, **2g**, **5a** and **5g** from molecular dynamics (MD) and ab initio (AI) calculations

Torsion	2a		2g	
	MD	AI	MD	AI
1	180	177	180	177
2	67, 108, −67	165	113, 68, −61	146
3	—	—	—	—
4	181, −74, −110	−71	−69, 179, 72	−67
5	—	—	—	—

	5a		5g	
1	180	178	180	179
2	178, 126, 52	172	−125, 190, 54	−167
3	62	51	−119	−122
4	176	173	175, 70	168
5	1	−1	1	0

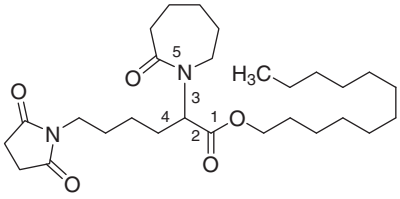

Figure 4. Designation of torsion angles.

angles from the molecular dynamics simulations are given in Table 3. For comparison, global minima from ab initio calculations are also shown. The designation of torsion angles is illustrated in Figure 4.

Molecular dynamics simulations confirm very frequent changes of torsion angles in the alkyl chain, especially for the dodecyl ester where the conformer life-times are of the order of only picoseconds. Torsion angles of the hexanoate chain change at least one order less frequently than of the alkyl chain. The azepan ring preserves its chair conformation and is planar at torsion angle 5. It is interesting that this torsion angle is not more constrained than other torsion angles within the ring. On the other hand, it was observed that the presence of the azepan ring significantly constrains torsion angle 4 in compounds **5a** and **5g**. Otherwise, there were only minor differences between all studied compounds.

Both ab initio calculations and molecular dynamics simulations predict the non-planar conformation of the studied compounds. However, the conformations of the alkyl and hexanoate chains can change almost freely according to molecular dynamics simulations. Comparing the 'Azone sub-structure' of the compounds, **5a** and **5g**, with Azone itself (Fig. 1), the most significant difference is the presence of the ester group which, owing to its rigid planar structure, prevents the adoption of the 'soup-spoon'-like conformation described by Hoogstraate et al.[33] It is unlikely that molecules, **5a** and **5g**, are able to intercalate with cholesterol in the stratum corneum,[34] as, based on in silico calculations using HyperChem,[35] the hexyl chain in **5a** (~8 Å) is too short and the dodecyl chain in **5g** (12 Å) is too long compared to the cholesterol steroidal skeleton, which is about 10 Å.[34]

2.5. In vitro screening of transdermal penetration-enhancing activity

By using theophylline as a model penetrant, we evaluated the penetration-enhancing activity of the prepared compounds using static Franz diffusion cells,[19] with propylene glycol/water (1:1 v/v) as a donor vehicle. Control experiments used theophylline in the donor vehicle in the absence of any enhancer. Due to its medium polarity ($\log P$ −0.06; $\log D_8$ −0.05),[42,43] theophylline has been used as a model drug and has been widely utilized in transdermal penetration experiments.[44,45] The majority of our studies used propylene glycol or a propylene glycol mixture with water or ethanol as a donor vehicle. While other studies have demonstrated that propylene glycol alone (or a propylene glycol/water co-solvent system) does not alter membranes, propylene glycol plays a synergistic role in combination with other chemical penetration enhancers.[46–48] For the initial evaluation of the enhancement activity of the prepared compounds, porcine ear skin was chosen as this tissue is a suitable alternative to human skin.[49,50] Importantly, porcine skin is known to be biochemically and histologically similar to that of humans, with full-thickness pig ear skin being used in a number of percutaneous absorption studies.[51] On the other hand, dermatomed skin has been recommended for examining hydrophobic penetrants.[52]

The ability of our alkyl esters, **2a**–**g** and **5a–g**, to enhance the penetration of theophylline through porcine skin, in comparison to oleic acid (OA), is illustrated in Figure 5. Oleic acid was used as a standard enhancer as it is one of most characterized enhancers in the fatty acid group.[53] Our synthesized enhancers, **2a**–**g** and **5a–g**, increased the penetration of theophylline through porcine skin, demonstrating higher enhancement ratios than OA, which are presented in Table 1. According to the results, it can be stated that the alkyl-6-(2,5-dioxopyrrolidin-1-yl)hexanoates (**2a–g**) expressed higher enhancement ratios than the alkyl-6-(2,5-dioxopyrrolidin-1-yl)-2-(2-oxoazepan-1-yl)hexanoates (**5a**–**g**). Within the 6-(2,5-dioxopyrrolidin-1-yl)hexanoates (**2**) the highest enhancement ratios were demonstrated by compounds **2e** (decyl), **2f** (undecyl) and **2d** (nonyl), with enhancement ratios of 3.54, 3.51 and 3.14, respectively. Dodecyl-6-(2,5-dioxopyrrolidin-1-yl)-2-(2-oxoazepan-1-yl)hexanoate (**5g**) showed the highest enhancement ratios within the azepan-2-one series (**5**), with an enhancement ratio value of 2.48. The chain length of the most active compounds **2d**–**g** (C_9-C_{11}) corresponds to the molecular length of sphingolipids and/or cholesterol derivatives, see Section 2.4 and Brain and Walters.[34]

Our current data (Table 1; Fig. 5) suggests that our 6-(2,5-dioxopyrrolidin-1-yl)hexanoates (**2**) and azepan-2-one (**5**) series of compounds show moderate penetration activity. Interestingly, the compounds within series **2** showed the highest enhancement ratios of all the substituted 6-aminohexanoates transdermal enhancers yet synthesized.[11,12] Their moderate activity may be explained considering the 3D structures of the mentioned transdermal enhancers (Figs. 2 and 3), where the non-planar (coned/coiled) conformations of the compounds are favored. It can be predicted that their intercalation potency in skin is decreased due to their non-planar, contrary to planar (open) conformations, the latter of which can increase penetration activity.[3,7] As described above in Section 2.4, the absence of the 'soup-spoon'-like conformation of the azepanone ring in compounds **5a**–**g** could be responsible for the observed decrease in enhancement activity.[3,32–34]

Generally, it can be stated that compounds without the $C_{(2)}$ substitution (C_{10} ester chain **2e**, enhancement ratio = 3.54 and C_{11} ester chain **2f**, enhancement ratio = 3.51) were the most active followed by seven-membered compounds (C_{12} ester chain **5g**, enhancement ratio = 2.48). The rest of the alkyl-6-(2,5-dioxopyrrolidin-1-yl)-2-(substituted)hexanoates showed lower activity. Depending on the substitution by a heterocycle at the α carbon, the compounds including nonyl to dodecyl alkyl chains were the most effective in a particular series. In the study dealing with six-membered *N*-heterocycles (piperidin-2-one or morpholin-4-yl were $C_{(2)}$ substituents), the highest enhancement ratios were exhibited by undecyl-6-(2,5-dioxopyrrolidin-1-yl)-2-(2-oxopiperidin-1-yl)hexanoates (enhancement ratio = 2.36), while the series with morpholine showed slightly lower activities.[12] In a series

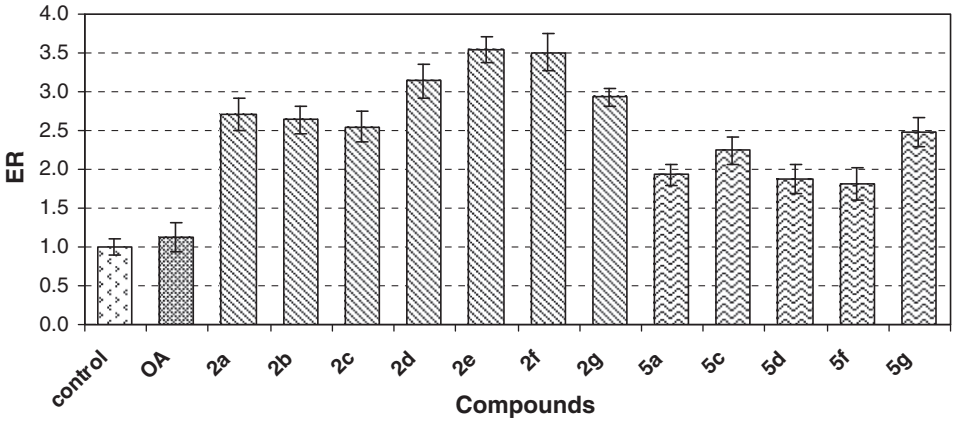

Figure 5. Enhancement ratios (ERs) of the prepared compounds **2a–g**, **5a–g** and oleic acid (OA). Control experiments used theophylline in the donor vehicle without any enhancer. Results are expressed as mean ± SD (n = 3 experiments).

of alkyl-6-(2,5-dioxopyrrolidin-1-yl)-2-(2-oxopyrrolidin-1-yl)hexanoates, the highest enhancement ratios were exhibited by the nonyl ester chain (enhancement ratio = 2.45).[11] The significantly lower activities of $C_{(2)}$ substituted derivatives can be caused by the 'non-soup-spoon'-like conformations of the *N*-heterocyclic rings.

The ability of the enhancers to penetrate through the skin was also investigated. None of the compounds were detected in the receptor compartment after 24 h and it was assumed that they did not penetrate through the skin barrier or remained incorporated in skin structures due to their high lipophilicity. This may be advantageous, because their entrance into the systemic circulation and potential toxicity is prevented.

3. Conclusions

We prepared a series of seven alkyl-6-(2,5-dioxopyrrolidin-1-yl)hexanoates and seven alkyl-6-(2,5-dioxopyrrolidin-1-yl)-2-(2-oxoazepan-1-yl)hexanoates containing C_6–C_{12} linear alkyl ester chains as novel penetration enhancers. Theophylline was used as a model penetrant to assess the ability of the compounds to enhance transdermal penetration. Although all compounds showed higher enhancement ratios than oleic acid, none of the prepared compounds were able to penetrate through the skin.

The compounds that had the highest enhancement ratios in this study were **2e** (C_{10} ester chain) and **2f** (C_{11} ester chain). It can be concluded that the series non-substituted in the $C_{(2)}$ position by a ω-lactam ring, **2a–g**, showed significantly higher activities than those with azepan-2-one, **5a–g**. Additionally, the anti-proliferative activity of these compounds was evaluated against human cancer cells (SK-N-MC neuroepithelioma) in culture and none of the analogs demonstrated any marked anti-proliferative activity. This suggests that these novel penetration enhancers would have minimal side-effects when topically administered. In summary, the novel analogs, **2e** and **2f**, are promising lead compounds as potential chemical penetration enhancers.

4. Experimental

4.1. Chemistry

Reagents were purchased from Merck (Darmstadt, Germany) and Sigma–Aldrich (Schnelldorf, Germany). For column chromatography, Kieselgel 60, 0.040–0.063 mm (Merck, Darmstadt, Germany) was used. Alumina-backed silica gel 40 F254 plates (Merck, Darmstadt, Germany) were implemented for thin layer chromatography (TLC) experiments and the plates were examined under UV (254 nm) and evaluated in iodine vapour. The uncorrected melting points were determined on a Boetius PHMK apparatus (Nagema, Germany). Infrared (IR) spectra were recorded on a Smart MIRacle™ ATR ZnSe for Nicolet™ 6700 FT-IR Spectrometer (Thermo Scientific, USA). The spectra were obtained in the 4000–600 cm^{-1} region by accumulation of 256 scans with a resolution of 2 cm^{-1}. A Bruker Avance-500 FT-NMR spectrometer was used to record the ^1H and ^{13}C NMR spectra (500 MHz for ^1H and 125 MHz for ^{13}C, Bruker Comp., Karlsruhe, Germany). $Si(CH_3)_4$ was used as an internal reference and chemicals shifts are reported in ppm (δ). Diffuse and easily exchangeable signals were omitted. A LTQ Orbitrap Hybrid Mass Spectrometer (Thermo Electron Corporation, USA) was employed to record mass spectra using direct injection into an APCI source (400 °C) in the positive mode.

4.1.1. 6-(2,5-Dioxopyrrolidin-1-yl)hexanoic acid (1)

This compound was synthesised as described previously by Brychtova et al.[11,12,23,24]

4.1.2. General procedure for preparation alkyl-6-(2,5-dioxopyrrolidin-1-yl)hexanoates (2a–g)

A mixture of organic acid **1** (4.69 mmol), *N,N′*-dicyclohexylcarbodiimide (5.16 mmol), appropriate primary alcohol (9.38 mmol) and a catalytic amount of 4-(dimethylamino)pyridine (0.47 mmol) in dry dichloromethane (15 mL) was stirred at room temperature under a nitrogen atmosphere overnight. The resulting precipitate of *N,N′*-dicyclohexylurea was filtered off. The filtrate was evaporated and the residue was purified by column chromatography on silica gel using ethyl acetate/petroleum ether (1:2) as the eluent.

4.1.3. Hexyl-6-(2,5-dioxopyrrolidin-1-yl)hexanoate (2a)

Colourless oil. Yield: 54%. IR (cm^{-1}): 2929, 2856, 1730, 1698, 1401, 1143. ^1H NMR (500 MHz, $CDCl_3$), δ: 3.99 (t, J = 6.7 Hz, 2H, $COOCH_2$), 3.44 (t, J = 7.3 Hz, 2H, NCH_2), 2.65 (s, 4H, $OCCH_2CH_2CO$), 2.23 (t, J = 7.4 Hz, 2H, CH_2COO), 1.66–1.46 (m, 6H, CH_2), 1.40–1.18 (m, 8H, CH_2), 0.83 (t, J = 6.5 Hz, 3H, CH_3). ^{13}C NMR (125 MHz, $CDCl_3$), δ: 177.08, 173.38, 64.34, 38.45, 33.95, 31.28, 28.46, 28.03, 27.22, 26.21, 25.44, 24.33, 22.39, 13.85. HR-MS: for $C_{16}H_{28}NO_4$ $[M+H]^+$ calculated 298.2013 m/z, found 298.2012 m/z.

4.1.4. Heptyl-6-(2,5-dioxopyrrolidin-1-yl)hexanoate (2b)

Colourless oil. Yield: 51%. IR (cm^{-1}): 2929, 2857, 1730, 1698, 1401, 1142. ^1H NMR (500 MHz, $CDCl_3$), δ: 4.04 (t, J = 6.7 Hz, 2H, $COOCH_2$), 3.49 (t, J = 7.3 Hz, 2H, NCH_2), 2.69 (s, 4H, $OCCH_2CH_2CO$), 2.28 (t, J = 7.4 Hz, 2H, CH_2COO), 1.71–1.49 (m, 6H, CH_2), 1.38–1.18

(m, 10H, CH_2), 0.87 (t, J = 6.6 Hz, 3H, CH_3). ^{13}C NMR (125 MHz, $CDCl_3$), δ: 177.48, 173.56, 64.50, 38.60, 34.07, 31.68, 28.87, 28.61, 28.13, 27.32, 26.33, 25.85, 24.44, 14.02. HR-MS: for $C_{17}H_{30}NO_4$ $[M+H]^+$ calculated 312.2969 m/z, found 312.2969 m/z.

4.1.5. Octyl-6-(2,5-dioxopyrrolidin-1-yl)hexanoate (2c)

Colourless oil. Yield: 58%. IR (cm^{-1}): 2928, 2856, 1730, 1698, 1401, 1142. ^{1}H NMR (500 MHz, $CDCl_3$), δ: 4.01 (t, J = 6.7 Hz, 2H, $COOCH_2$), 3.46 (t, J = 7.3 Hz, 2H, NCH_2), 2.66 (s, 4H, $OCCH_2CH_2CO$), 2.25 (t, J = 7.4 Hz, 2H, CH_2COO), 1.64–1.46 (m, 6H, CH_2), 1.35–1.18 (m, 12H, CH_2), 0.84 (t, J = 6.5 Hz, 3H, CH_3). ^{13}C NMR (125 MHz, $CDCl_3$), δ: 177.14, 173.49, 64.45, 38.57, 34.04, 31.76, 29.13, 28.60, 28.11, 27.29, 26.31, 25.87, 24.34, 13.99. HR-MS: for $C_{18}H_{32}NO_4$ $[M+H]^+$ calculated 326.2326 m/z, found 326.2327 m/z.

4.1.6. Nonyl-6-(2,5-dioxopyrrolidin-1-yl)hexanoate (2d)

Colourless oil. Yield: 48%. IR (cm^{-1}): 2926, 2855, 1730, 1699, 1401, 1143. ^{1}H NMR (500 MHz, $CDCl_3$), δ: 4.03 (t, J = 6.7 Hz, 2H, $COOCH_2$), 3.48 (t, J = 7.3 Hz, 2H, NCH_2), 2.68 (s, 4H, $OCCH_2CH_2CO$), 2.27 (t, J = 7.4 Hz, 2H, CH_2COO), 1.70–1.49 (m, 6H, CH_2), 1.38–1.21 (m, 14H, CH_2), 0.86 (t, J = 6.3 Hz, 3H, CH_3). ^{13}C NMR (125 MHz, $CDCl_3$), δ: 177.11, 173.47, 64.46, 38.58, 34.06, 31.81, 29.43, 29.19, 28.61, 28.12, 27.32, 26.33, 25.88, 24.43, 22.61, 14.03. HR-MS: for $C_{19}H_{34}NO_4$ $[M+H]^+$ calculated 340.2482 m/z, found 340.2482 m/z.

4.1.7. Decyl-6-(2,5-dioxopyrrolidin-1-yl)hexanoate (2e)

Colourless oil. Yield: 54%. IR (cm^{-1}): 2925, 2854, 1731, 1699, 1401, 1143. ^{1}H NMR (500 MHz, $CDCl_3$), δ: 4.03 (t, J = 6.7 Hz, 2H, $COOCH_2$), 3.49 (t, J = 7.3 Hz, 2H, NCH_2), 2.69 (s, 4H, $OCCH_2CH_2CO$), 2.27 (t, J = 7.41 Hz, 2H, CH_2COO), 1.70–1.50 (m, 6H, CH_2), 1.42–1.21 (m, 16H, CH_2), 0.86 (t, J = 6.4 Hz, 3H, CH_3). ^{13}C NMR (125 MHz, $CDCl_3$), δ: 177.08, 173.45, 64.46, 38.59, 34.07, 31.85, 29.48, 29.24, 28.64, 28.13, 27.32, 26.34, 25.90, 24.45, 22.62, 14.02. HR-MS: for $C_{20}H_{36}NO_4$ $[M+H]^+$ calculated 354.2639 m/z, found 354.2638 m/z.

4.1.8. Undecyl-6-(2,5-dioxopyrrolidin-1-yl)hexanoate (2f)

Colourless oil. Yield: 49%. IR (cm^{-1}): 2924, 2854, 1731, 1699, 1401, 1143. ^{1}H NMR (500 MHz, $CDCl_3$), δ: 4.05 (t, J = 6.7 Hz, 2H, $COOCH_2$), 3.50 (t, J = 7.3 Hz, 2H, NCH_2), 2.70 (s, 4H, $OCCH_2CH_2CO$), 2.29 (t, J = 7.4 Hz, 2H, CH_2COO), 1.72–1.52 (m, 6H, CH_2), 1.40–1.17 (m, 18H, CH_2), 0.88 (t, J = 6.3 Hz, 3H, CH_3). ^{13}C NMR (125 MHz, $CDCl_3$), δ: 177.14, 173.52, 64.50, 38.62, 34.09, 31.89, 29.57, 29.50, 29.30, 29.24, 28.64, 28.15, 27.35, 26.36, 25.92, 24.47, 22.66, 14.08. HR-MS: for $C_{21}H_{38}NO_4$ $[M+H]^+$ calculated 368.2795 m/z, found 368.2796 m/z.

4.1.9. Dodecyl-6-(2,5-dioxopyrrolidin-1-yl)hexanoate (2g)

Colourless oil. Yield: 52%. IR (cm^{-1}): 2923, 2853, 1731, 1699, 1401, 1143. ^{1}H NMR (500 MHz, $CDCl_3$), δ: 4.05 (t, J = 6.7 Hz, 2H, $COOCH_2$), 3.50 (t, J = 7.4 Hz, 2H, NCH_2), 2.70 (s, 4H, $OCCH_2CH_2CO$), 2.29 (t, J = 7.4 Hz, 2H, CH_2COO), 1.72–1.52 (m, 6H, CH_2), 1.40–1.16 (m, 20H, CH_2), 0.88 (t, J = 6.4 Hz, 3H, CH_3). ^{13}C NMR (125 MHz, $CDCl_3$), δ: 177.12, 173.49, 64.48, 38.60, 34.07, 31.88, 29.60, 29.54, 29.49, 29.30, 29.23, 28.63, 28.13, 27.33, 26.34, 25.91, 24.45, 22.65, 14.06. HR-MS: for $C_{22}H_{40}NO_4$ $[M+H]^+$ calculated 382.2952 m/z, found 382.2952 m/z.

4.1.10. Ethyl-2-bromo-6-(2,5-dioxopyrrolidin-1-yl)hexanoate (3)

This compound was synthesised as described by Brychtova et al.[11,12,23,24]

4.1.11. Ethyl-6-(2,5-dioxopyrrolidin-1-yl)-2-(2-oxoazepan-1-yl)hexanoate (4)

Azepan-2-one (46.9 mmol) was slowly added to a suspension of NaH (51.5 mmol, 60% dispersion in mineral oil) in dry DMF (100 mL). The mixture was stirred until the evolution of hydrogen gas ceased. Compound **3** (10.0 g, 31.2 mmol) and Cu_2O (1.1 g, 7.8 mmol) were then added and the mixture was refluxed for 9 h under argon. The mixture was allowed to cool and was poured onto ice, filtered and extracted with chloroform. The combined organic extracts were washed with water, dried over $MgSO_4$, filtered and the organic solvent was removed under vacuum. The crude product was purified by flash chromatography on silica gel (ethyl acetate/petroleum ether/TEA 10:1:0.1). This provided light yellow oil. Yield: 65%. IR (cm^{-1}): 2937, 2863, 1731, 1698, 1643, 1401, 1156. ^{1}H NMR (500 MHz, $CDCl_3$), δ: 5.10 (dd, J^1 = 9.9 Hz, J^2 = 5.1 Hz, 1H, CH), 4.33–4.00 (m, 2H, OCH_2), 3.50 (t, J = 7.2 Hz, 2H, NCH_2), 3.41–3.15 (m, 2H, NCH_2 azep.), 2.71 (s, 4H, $OCCH_2CH_2$-CO), 2.64–2.51 (m, 2H, $OCCH_2$ azep.), 2.05–1.90 (m, 2H, CH_2), 1.85–1.45 (m, 8H, CH_2), 1.39–1.27 (m, 2H, CH_2), 1.26 (t, J = 6.6 Hz, 3H, CH_3). ^{13}C NMR (125 MHz, $CDCl_3$), δ: 177.18, 176.22, 171.47, 60.97, 57.06, 46.19, 38.41, 37.28, 29.91, 28.63, 28.11, 27.29, 23.46, 23.25, 14.12. HR-MS: for $C_{18}H_{29}N_2O_5$ $[M+H]^+$ calculated 353.2071 m/z, found 353.2071 m/z.

4.1.12. General procedure for preparation alkyl-6-(2,5-dioxopyrrolidin-1-yl)-2-(2-oxoazepan-1-yl)hexanoates (5a–g)

A mixture of the ethyl ester **4** (7.7 mmol), appropriate primary alcohol (38.5 mmol) and metallic sodium (3.85 mmol) was stirred at 90 °C in an oil bath until sodium was completely dissolved. The mixture was then heated at 130 °C for 5–7 h and the ethanol formed during the reaction was removed by distillation. Any excess of the longer-chain alkyl alcohol was distilled under reduced pressure and the remainder was extracted with acetic acid (0.5 M) and diethylether, with the organic layer dried over $MgSO_4$, filtered and evaporated. The crude product was purified by column chromatography on silica gel using ethyl acetate/petroleum ether/TEA (10:1:0.1) as the eluent.

4.1.13. Hexyl-6-(2,5-dioxopyrrolidin-1-yl)-2-(2-oxoazepan-1-yl)hexanoate (5a)

Light yellow oil. Yield: 20%. IR (cm^{-1}): 2930, 2858, 1731, 1698, 1643, 1401, 1157. ^{1}H NMR (500 MHz, $CDCl_3$), δ: 5.10 (dd, J^1 = 9.8 Hz, J^2 = 5.2 Hz, 1H, CH), 4.07 (t, J = 6.7 Hz, 2H, OCH_2), 3.50 (t, J = 7.2 Hz, 2H, NCH_2), 3.41–3.14 (m, 2H, NCH_2 azep.), 2.70 (s, 4H, $OCCH_2CH_2CO$), 2.63–2.52 (m, 2H, $OCCH_2$ azep.), 2.05–1.50 (m, 12H, CH_2), 1.44–1.22 (m, 8H, CH_2), 0.89 (t, J = 6.4 Hz, 3H, CH_3). ^{13}C NMR (125 MHz, $CDCl_3$), δ: 177.20, 176.25, 171.60, 65.23, 57.09, 46.22, 38.46, 37.33, 31.34, 29.97, 28.69, 28.59, 28.48, 28.16, 27.35, 25.55, 23.52, 23.30, 22.48, 13.94. HR-MS: for $C_{22}H_{37}N_2O_5$ $[M+H]^+$ calculated 409.2697 m/z, found 409.2697 m/z.

4.1.14. Heptyl-6-(2,5-dioxopyrrolidin-1-yl)-2-(2-oxoazepan-1-yl)hexanoate (5b)

Light yellow oil. Yield: 25%. IR (cm^{-1}): 2928, 2856, 1733, 1698, 1643, 1401, 1157. ^{1}H NMR (500 MHz, $CDCl_3$), δ: 5.11 (dd, J^1 = 9.9 Hz, J^2 = 5.1 Hz, 1H, CH), 4.07 (t, J = 6.7 Hz, 2H, OCH_2), 3.50 (t, J = 7.2 Hz, 2H, NCH_2), 3.41–3.14 (m, 2H, NCH_2 azep.), 2.70 (s, 4H, $OCCH_2CH_2CO$), 2.63–2.52 (m, 2H, $OCCH_2$ azep.), 2.05–1.50 (m, 12H, CH_2), 1.44–1.22 (m, 10H, CH_2), 0.88 (t, J = 6.4 Hz, 3H, CH_3). ^{13}C NMR (125 MHz, $CDCl_3$), δ: 177.21, 176.25, 171.61, 65.23, 57.08, 46.22, 38.46, 37.33, 31.38, 29.85, 28.69, 28.59, 28.48, 28.16, 27.35, 25.55, 23.52, 23.31, 22.52, 13.99. HR-MS: for $C_{23}H_{39}N_2O_5$ $[M+H]^+$ calculated 423.2853 m/z, found 423.2854 m/z.

4.1.15. Octyl-6-(2,5-dioxopyrrolidin-1-yl)-2-(2-oxoazepan-1-yl)hexanoate (5c)

Light yellow oil. Yield: 23%. IR (cm^{-1}): 2926, 2856, 1731, 1698, 1643, 1401, 1157. ^{1}H NMR (500 MHz, $CDCl_3$), δ: 5.11 (dd, J^1 = 9.9 Hz, J^2 = 5.1 Hz, 1H, CH), 4.07 (t, J = 6.7 Hz, 2H, OCH_2), 3.50 (t, J = 7.2 Hz, 2H, NCH_2), 3.41–3.16 (m, 2H, NCH_2 azep.), 2.70 (s,

4H, $OCCH_2CH_2CO$), 2.63–2.51 (m, 2H, $OCCH_2$ azep.), 2.05–1.50 (m, 12H, CH_2), 1.41–1.21 (m, 12H, CH_2), 0.88 (t, J = 6.4 Hz, 3H, CH_3). ^{13}C NMR (125 MHz, $CDCl_3$), δ: 177.20, 176.25, 171.61, 65.24, 57.09, 46.23, 38.47, 37.33, 31.75, 29.98, 29.13, 28.70, 28.53, 28.16, 27.36, 25.89, 23.53, 23.31, 22.60, 14.04. HR-MS: for $C_{24}H_{41}N_2O_5$ $[M+H]^+$ calculated 437.3010 m/z, found 437.3012 m/z.

4.1.16. Nonyl-6-(2,5-dioxopyrrolidin-1-yl)-2-(2-oxoazepan-1-yl)hexanoate (5d)

Light yellow oil. Yield: 18%. IR (cm^{-1}): 2925, 2856, 1731, 1698, 1643, 1401, 1157. ^1H NMR (500 MHz, $CDCl_3$), δ: 5.10 (dd, J^1 = 9.9 Hz, J^2 = 5.1 Hz, 1H, CH), 4.07 (t, J = 6.7 Hz, 2H, OCH_2), 3.50 (t, J = 7.2 Hz, 2H, NCH_2), 3.41–3.16 (m, 2H, NCH_2 azep.), 2.70 (s, 4H, $OCCH_2CH_2CO$), 2.64–2.49 (m, 2H, $OCCH_2$ azep.), 2.05–1.48 (m, 12H, CH_2), 1.45–1.18 (m, 14H, CH_2), 0.88 (t, J = 6.4 Hz, 3H, CH_3). ^{13}C NMR (125 MHz, $CDCl_3$), δ: 177.17, 176.21, 171.58, 65.21, 57.08, 46.21, 38.44, 37.31, 31.80, 29.95, 29.41, 29.16, 28.68, 28.52, 28.14, 27.33, 25.87, 23.51, 23.29, 22.61, 14.03. HR-MS: for $C_{25}H_{43}N_2O_5$ $[M+H]^+$ calculated 451.3166 m/z, found 451.3166 m/z.

4.1.17. Decyl-6-(2,5-dioxopyrrolidin-1-yl)-2-(2-oxoazepan-1-yl)hexanoate (5e)

Light yellow oil. Yield: 18%. IR (cm^{-1}): 2924, 2854, 1731, 1698, 1643, 1401, 1157. ^1H NMR (500 MHz, $CDCl_3$), δ: 5.10 (dd, J^1 = 9.9 Hz, J^2 = 5.2 Hz, 1H, CH), 4.07 (t, J = 6,7 Hz, 2H, OCH_2), 3.50 (t, J = 7.2 Hz, 2H, NCH_2), 3.40–3.16 (m, 2H, NCH_2 azep.), 2.70 (s, 4H, $OCCH_2CH_2CO$), 2.63–2.51 (m, 2H, $OCCH_2$ azep.), 2.02–1.50 (m, 12H, CH_2), 1.46–1.19 (m, 16H, CH_2), 0.88 (t, J = 6.4 Hz, 3H, CH_3). ^{13}C NMR (125 MHz, $CDCl_3$), δ: 177.18, 176.23, 171.60, 65.24, 57.10, 46.23, 38.47, 37.34, 31.86, 29.98, 29.49, 29.26, 29.18, 28.71, 28.54, 28.16, 27.36, 25.90, 23.53, 23.32, 22.64, 14.06. HR-MS: for $C_{26}H_{45}N_2O_5$ $[M+H]^+$ calculated 465.3323 m/z, found 465.3324 m/z.

4.1.18. Undecyl-6-(2,5-dioxopyrrolidin-1-yl)-2-(2-oxoazepan-1-yl)hexanoate (5f)

Light yellow oil. Yield: 15%. IR (cm^{-1}): 2924, 2854, 1731, 1698, 1643, 1401, 1157. ^1H NMR (500 MHz, $CDCl_3$), δ: 5.10 (dd, J^1 = 9.9 Hz, J^2 = 5.1 Hz, 1H, CH), 4.07 (t, J = 6.7 Hz, 2H, OCH_2), 3.50 (t, J = 7.2 Hz, 2H, NCH_2), 3.41–3.16 (m, 2H, NCH_2 azep.), 2.70 (s, 4H, $OCCH_2CH_2CO$), 2.61–2.49 (m, 2H, $OCCH_2$ azep.), 2.02–1.50 (m, 12H, CH_2), 1.42–1.17 (m, 18H, CH_2), 0.88 (t, J = 6.4 Hz, 3H, CH_3).^{13}C NMR (125 MHz, $CDCl_3$), δ: 177.20, 176.24, 171.61, 65.24, 57.10, 46.23, 38.47, 37.34, 31.88, 29.98, 29.55, 29.49, 29.30, 29.19, 28.71, 28.54, 28.16, 27.36, 25.90, 23.53, 23.32, 22.65, 14.07. HR-MS: for $C_{27}H_{47}N_2O_5$ $[M+H]^+$ calculated 479.3479 m/z, found 479.3480 m/z.

4.1.19. Dodecyl-6-(2,5-dioxopyrrolidin-1-yl)-2-(2-oxoazepan-1-yl)hexanoate (5g)

Light yellow oil. Yield: 16%. IR (cm^{-1}): 2924, 2854, 1731, 1698, 1643, 1401, 1157. ^1H NMR (500 MHz, $CDCl_3$), δ: 5.10 (dd, J^1 = 9.8 Hz, J^2 = 5.1 Hz, 1H, CH), 4.07 (t, J = 6.6 Hz, 2H, OCH_2), 3.50 (t, J = 7.1 Hz, 2H, NCH_2), 3.40–3.17 (m, 2H, NCH_2 azep.), 2.70 (s, 4H, O=CCH_2CH_2C=O), 2.62–2.49 (m, 2H, O=CCH_2 azep.), 2.04–1.48 (m, 12H, CH_2), 1.42–1.15 (m, 20H, CH2), 0.88 (t, J = 6.2 Hz, 3H, CH_3). ^{13}C NMR (125 MHz, $CDCl_3$), δ: 177.18, 176.23, 171.61, 65.25, 57.11, 46.23, 38.47, 37.34, 31.89, 29.98, 29.62, 29.56, 29.49, 29.32, 29.20, 28.71, 28.55, 28.17, 27.36, 25.90, 23.54, 23.32, 22.66, 14.07. HR-MS: for $C_{28}H_{49}N_2O_5$ $[M+H]^+$ calculated 493.3636 m/z, found 493.3636 m/z.

4.2. Lipophilicity determination using HPLC (capacity factor k/calculated log$k$)

The capacity factor, k, was determined as previously described,[12] using an Agilent 1200 series HPLC system equipped with an automatic injector, a C_{18} 5 μm, 4.6 × 150 mm Zorbax Eclipse XDB chromatographic column, a diode array detection (DAD) system and a quaternary model pump (Agilent Technologies, Germany). The ChemStation chromatography software was used for data acquisition. A mixture of MeOH (HPLC grade, 85.0%) and H_2O (HPLC grade, 15.0%) was used as the mobile phase. A total flow of 0.4 mL/min was used, while an injection volume of 10 μL and column temperature of 25 °C were employed. A detection wavelength of 204 nm and the bandwidth of 8 nm were chosen. A KI methanolic solution was used to determine the dead time (t_D) and retention times (t_R) were measured in minutes.

ChemStation Chromatography Software (Agilent Technologies, Germany) was used to calculate the capacity factor, k, according to the formula $k = (t_R - t_D)/t_D$, where t_R is the solute retention time, t_D denotes the dead time obtained via an unretained analyte. The log$k$ values, calculated from the capacity factors, k, were used as an index of lipophilicity converted to the log$P$ scale.[18]

4.3. Cell culture and in vitro anti-proliferative activity

The human SK-N-MC neuroepithelioma cell line was obtained from the American Type Culture Collection (Manassas, VA, USA). This cell type was cultured using minimum essential medium (MEM; Gibco, Melbourne, Australia) containing 10% (v/v) FBS, 1% (v/v) non-essential amino acids (Gibco), 1% (v/v) streptomycin (Gibco), 1 mM sodium pyruvate (Gibco), 2 mM L-glutamine (Gibco), 100 U/mL penicillin (Gibco) and 0.28 μg/mL fungizone (Squibb Pharmaceuticals, Montreal, Canada). Cells were cultured under standard conditions at 37 °C in a humidified atmosphere of 5% CO_2 and 95% air.

The effect of the compounds on cellular proliferation was examined using the MTT [1-(4,5-dimethylthiazol-2-yl)-2,5-diphenyl tetrazolium] assay by standard techniques.[29,30] MTT reduction is proportional to viable cell counts using SK-N-MC cells.[31] SK-N-MC cells were seeded at 1.5 × 10^4 cells/well in 96-well microtiter plates in medium containing the compounds (0–25 μM) and human diferric transferrin (Tf) at 1.25 μM ([Fe] = 2.5 μM). Control samples contained Tf (1.25 μM) in the absence of the compounds. As their anti-proliferative activity is well characterized in this cell line, the chelators, DFO and Dp44mT, were also included as positive control compounds.[29,30] The cells were incubated at 37 °C for 72 h, afterwards 10 μL of MTT solution (stock solution: 5 mg/mL) was added to each well and incubated for 2 h/37 °C. After cell solubilization using 100 μL of 10% SDS–50% isobutanol in 0.01 M HCl, the plates were read at 570 nm using a scanning multi-well spectrophotometer. The inhibitory concentration (IC_{50}) was defined as the concentration of compound necessary to reduce the absorbance to 50% of the untreated control.

4.4. Lipophilicity and geometry calculations

Log$P$ values (i.e., the logarithm of the n-octanol/water partition coefficient) were predicted using CS ChemOffice Ultra 10.0[26] and ACD/LogP DB software.[27] *C*log$P$ values (the logarithm of n-octanol/water partition coefficient based on established chemical interactions) were also generated using CS ChemOffice Ultra 10.0[26] software. The results are shown in Table 1.

The initial scan of geometries was performed using the conformational search utility in HyperChem.[35] Structures within 2 kcal/mol were then re-optimized in water at HF/4–31G ab initio level in Gaussian 09W[36] Water was simulated using the CPCM polarizable continuum solvation model.[54] The resulting low-energy conformations (11–50) were used for final optimizations including the correlation energy at B3PW91/6–31G level, again in implicit water. These results are illustrated in Figures 2 and 3 and shown in Table 2.

Molecular dynamics simulations were performed in HyperChem using the MM+ force field. A periodic box with dimensions $a = b = c = 20$ Å was filled with solvent molecules using a published method[55] and adjusted using our own code. The resulting system consisted of 15 molecules of (*R*)-propylene glycol, 15 molecules of the (*S*)-enantiomer, 120 molecules of water and a solute molecule. The resulting macroscopic density was 1.02 g/cm^3. Data generated from molecular dynamics simulations were accumulated from a series of 500 ps runs with a 1 fs time step at 298 K within a thermostatically controlled water bath. Data were collected every 100 steps. The results are shown in Table 3.

4.5. In vitro screening of transdermal penetration-enhancing activity

Full thickness dorsal skin from porcine ear was cut into pieces and stored at −20 °C until needed. Skin samples were slowly thawed (at 4 °C overnight and then at ambient temperature) prior to each experiment. The penetration-enhancing activity of the novel compounds **2a–g** and **5a–g** were evaluated using a vertical Franz diffusion cell (PermeGear Inc., USA), with a receptor volume of 5.2 mL and a donor surface area of 0.635 cm^2. The skin was mounted epidermal side up between the donor and receptor compartments of the diffusion cell. The receptor compartment was filled with phosphate buffered saline (pH 7.4) and maintained at 37 ± 0.5 °C using a circulating water bath. The receptor compartment was continuously stirred using a magnetic stirring bar. Prior to the experiment, the skin was kept in contact with the receptor phase for 0.5 h at 37 ± 0.5 °C. The donor samples were prepared by dissolving the enhancer (20 mg) in PG (0.5 mL) and a solution of theophylline (5 mg) in water (0.5 mL) was added. This mixture was shaken vigorously and then sonicated at 40 °C for 10 min. This stable system was applied to the skin surface and the donor compartment of the cell was covered by Parafilm®. The control samples were prepared in the same manner in the absence of the enhancers. Samples (0.5 mL) of the receptor phase were taken at 1, 2, 4, 8, 12 and 24 h and the cell was refilled with an equivalent volume of fresh buffer solution. For each compound, a minimum of three determinations were performed using skin fragments from a minimum of 2 animals. The samples were stored at −18 °C until analyzed by HPLC.

4.6. Sample analysis

Samples were analyzed for theophylline content from the transdermal penetration-enhancing activity studies described above using an Agilent 1200 series HPLC system equipped with a diode array detection (DAD) system, quaternary model pump and automatic injector (Agilent Technologies, Germany). ChemStation Chromatography Software was used for data acquisition. Acetonitrile (HPLC grade, 50.0%) and H_2O (HPLC grade, 50.0%) were used as the mobile phase. A Waters Symmetry, C_8 5 μm, 4.6 × 250 mm chromatographic column was used with a total flow of 0.5 mL/min, an injection volume of 10 μL and a column temperature of 25 °C. A detection wavelength of 280 nm with a bandwidth of 8 nm was chosen and a retention time (t_R) of 5.07 ± 0.05 min for theophylline was determined.

The cumulative amounts of theophylline that penetrated across the skin into the receptor compartment (μg/cm^2) were corrected for sample removal. These were plotted against time (h) and a linear dependence was found ($R^2 \geqslant 0.98$), while the steady state fluxes (μg/cm^2/h) were calculated using the linear region of the plots. Enhancement ratios were determined using the ratio of the flux of theophylline in the presence and absence of the enhancer. The results are summarized in Table 1.

The HPLC method described in Section 4.2 was employed for the determination of the penetrated enhancer using an injection volume of 10 μL. The samples of the receptor phase were withdrawn at the mentioned intervals and then subsequently analysed.

Acknowledgments

This study was supported by the Grant Agency of the Czech Republic (Czech Science Foundation), Project Number GACR P304/11/2246 and by the Ministry of Education of the Czech Republic MSM 6046137305. D.R.R. was supported by a NHMRC Senior Principal Research Fellowship and Project Grants and an ARC Discovery Grant. D.S.K. was supported by a Cancer Institute New South Wales Early Career Development Fellowship and Innovation Grant.

References and notes

1. *Percutaneous Penetration Enhancers*; Smith, E. W., Maibach, H. I., Eds., 2nd ed.; CRC Press: Boca Raton, FL, USA, 2006.
2. Thong, H.-Y.; Zhai, H.; Maibach, H. I. *Skin Pharmacol. Physiol.* **2007**, *20*, 272.
3. Jampilek, J.; Brychtova, K. *Med. Res. Rev.* doi: 10.1002/med.20227, in press.
4. Williams, A. C.; Barry, B. W. *Adv. Drug Deliv. Rev.* **2004**, *56*, 603.
5. Benson, H. A. E. *Curr. Drug Deliv.* **2005**, *2*, 23.
6. Sinha, V. R.; Kaur, M. P. *Drug Dev. Ind. Pharm.* **2000**, *26*, 1131.
7. Hadgraft, J.; Peck, J.; Williams, D. G.; Pugh, W. J.; Allan, G. *Int. J. Pharm.* **1996**, *141*, 17.
8. Lopez-Cervantes, M.; Marquez-Mejia, E.; Cazares-Delgadillo, J.; Quintanar-Guerrero, D.; Ganem-Quintanar, A.; Angeles-Anguiano, E. *Drug Dev. Ind. Pharm.* **2006**, *32*, 267.
9. Williams, A. C.; Barry, B. W. *Crit. Rev. Ther. Drug Carrier Syst.* **1992**, *9*, 305.
10. Pugh, W. J.; Wong, R.; Falson, F.; Michniak, B. B.; Moss, G. P. *J. Pharm. Pharmacol.* **2005**, *57*, 1389.
11. Brychtova, K.; Jampilek, J.; Opatrilova, R.; Raich, I.; Farsa, O.; Csollei, J. *Bioorg. Med. Chem.* **2010**, *18*, 73.
12. Brychtova, K.; Opatrilova, R.; Raich, I.; Kalinowski, D. S.; Dvorakova, L.; Placek, L.; Csollei, J.; Richardson, D. R.; Jampilek, J. *Bioorg. Med. Chem.* **2010**, *18*, 8556.
13. Zheng, T.; Hopfinger, A. J.; Esposito, E. X.; Liu, J.; Tseng, Y. J. *J. Chem. Inf. Model.* **2008**, *48*, 1238.
14. Ghafourian, T.; Zandasrar, P.; Hamishekar, H.; Nokhodchi, A. *J. Controlled Release* **2004**, *99*, 113.
15. Barry, B. W. *J. Controlled Release* **1987**, *6*, 85.
16. Kim, N.; El-Kattan, A. F.; Asbill, C. S.; Kennette, R. J.; Sowell, J. W.; Latour, R.; Michniak, B. B. *J. Controlled Release* **2001**, *73*, 183.
17. Baert, B.; Deconinck, E.; Van Gele, M.; Slodicka, M.; Stoppie, P.; Bode, S.; Slegers, G.; Vander Heyden, Y.; Lambert, J.; Beetens, J.; De Spiegeleer, B. *Bioorg. Med. Chem.* **2007**, *15*, 6943.
18. Pliska, V. Lipophilicity in Drug Action and Toxicology, 1st ed. In *Methods and Principles in Medicinal Chemistry*; Pliska, V., Testa, B., van der Waterbeemd, H., Eds.; Wiley-VCH: Weinheim, 1996; Vol. 4, pp 1–6.
19. Franz, T. J. *J. Invest. Dermatol.* **1975**, *64*, 190.
20. Lau, J.; Dorwald, F.Z.; Stephensen, H.; Bloch, P.; Hansen, T.K.; Madsen, K. PCT Int. Appl. 2006; WO/2006/097537.
21. Schwenk, E.; Papa, D. *J. Am. Chem. Soc.* **1948**, *70*, 3626.
22. Berry, J. P.; Isbell, A. F.; Hunt, G. E. *J. Org. Chem.* **1972**, *37*, 4396.
23. Brychtova, K.; Farsa, O.; Csollei, J. *Lett. Org. Chem.* **2009**, *6*, 25.
24. Brychtova, K.; Slaba, B.; Placek, L.; Jampilek, J.; Raich, I.; Csollei, J. *Molecules* **2009**, *14*, 3019.
25. Otera, J. *Chem. Rev.* **1993**, *93*, 1449. and references cited therein.
26. CS ChemOffice Ultra ver. 10.0, CambridgeSoft, Cambridge, MA, USA.
27. ACD/LogP DB software. ACD/Labs, ver. 11.01, Advanced Chemistry Development, Inc., Toronto, Canada, 2007.
28. Kalinowski, D. S.; Richardson, D. R. *Pharmacol. Rev.* **2005**, *57*, 547.
29. Richardson, D. R.; Sharpe, P. C.; Lovejoy, D. B.; Senaratne, D.; Kalinowski, D. S.; Islam, M.; Bernhardt, P. V. *J. Med. Chem.* **2006**, *49*, 6510.
30. Kalinowski, D. S.; Yu, Y.; Sharpe, P. C.; Islam, M.; Liao, Y.-T.; Lovejoy, D. B.; Kumar, N.; Bernhardt, P. V.; Richardson, D. R. *J. Med. Chem.* **2007**, *50*, 3716.
31. Richardson, D. R.; Tran, E. H.; Ponka, P. *Blood* **1995**, *86*, 4295.
32. Karande, P.; Jain, A.; Ergun, K.; Kispersky, V.; Mitragotri, S. *Proc. Natl. Acad. Sci. U.S.A.* **2005**, *102*, 4688.
33. Hoogstraate, A. J.; Verhoef, J.; Brussee, J.; Izerman, A. P.; Spies, F.; Boddé, H. E. *Int. J. Pharm.* **1991**, *76*, 37.
34. Brain, K. R.; Walters, K. A. Molecular modeling of skin permeation enhancement by chemical agents. In *Pharmaceutical Skin Penetration Enhancement*; Walters, K. A., Hadgraft, J., Eds.; Marcel Dekker: New York, 1993; pp 389–416.
35. HyperChem for Windows, ver. 8.0.3, Hypercube, Inc., Gainesville, FL, USA, 2007.
36. Frisch, M. J.; Trucks, G. W.; Schlegel, H. B.; Scuseria, G. E.; Robb, M. A.; Cheeseman, J. R.; Scalmani, G.; Barone, V.; Mennucci, B.; Petersson, G. A.; Nakatsuji, H.; Caricato, M.; Li, X.; Hratchian, H. P.; Izmaylov, A. F.; Bloino, J.; Zheng, G.; Sonnenberg, J. L.; Hada, M.; Ehara, M.; Toyota, K.; Fukuda, R.;

Hasegawa, J.; Ishida, M.; Nakajima, T.; Honda, Y.; Kitao, O.; Nakai, H.; Vreven, T., ; Montgomery, J. A., Jr.; Peralta, J. E.; Ogliaro, F.; Bearpark, M.; Heyd, J. J.; Brothers, E.; Kudin, K. N.; Staroverov, V. N.; Kobayashi, R.; Normand, J.; Raghavachari, K.; Rendell, A.; Burant, J. C.; Iyengar, S. S.; Tomasi, J.; Cossi, M.; Rega, N.; Millam, N. J.; Klene, M.; Knox, J. E.; Cross, J. B.; Bakken, V.; Adamo, C.; Jaramillo, J.; Gomperts, R.; Stratmann, R. E.; Yazyev, O.; Austin, A. J.; Cammi, R.; Pomelli, C.; Ochterski, J. W.; Martin, R. L.; Morokuma, K.; Zakrzewski, V. G.; Voth, G. A.; Salvador, P.; Dannenberg, J. J.; Dapprich, S.; Daniels, A. D.; Farkas, Ö.; Foresman, J. B.; Ortiz, J. V.; Cioslowski, J.; Fox, D. J. *Gaussian 09, Revision A.2*; Gaussian, Inc.: Wallingford, CT, USA, 2009.
37. Becke, A. D. *J. Chem. Phys.* **1993**, *98*, 5648.
38. Perdew, J. P.; Chevary, J. A.; Vosko, S. H.; Jackson, K. A.; Pederson, M. R.; Singh, D. J.; Fiolhais, C. *Phys. Rev. B: Condens. Matter* **1992**, *46*, 6671.
39. Hehre, W. J.; Ditchfield, R.; Pople, J. A. *J. Chem. Phys.* **1972**, *56*, 2257.
40. Davidson, E. R.; Feller, D. *Chem. Rev.* **1986**, *86*, 681.
41. Krack, M.; Köster, A. M. *J. Chem. Phys.* **1998**, *108*, 3226.
42. Ni, N.; El-Sayed, M. M.; Sanghvi, T.; Yalkowsky, S. H. *J. Pharm. Sci.* **2000**, *89*, 1620.
43. Katz, M.; Ben-Shlush, I.; Kolusheva, S.; Jelinek, R. *Pharm. Res.* **2006**, *23*, 580.
44. Fang, J. Y.; Tsai, T. H.; Hung, C. F.; Wong, W. W. *J. Pharm. Pharmacol.* **2004**, *56*, 1493.
45. Sloan, K. B.; Beall, H. D.; Taylor, H. E.; Getz, J. J.; Villaneuva, R.; Nipper, R.; Smith, K. *Int. J. Pharm.* **1998**, *171*, 185.
46. Evrard, D.; Touitou, E.; Kolusheva, S.; Fishov, Y.; Jelinek, R. *Pharm. Res.* **2001**, *18*, 943.
47. Williams, A. C.; Barry, B. W. *Int. J. Pharm.* **1989**, *56*, 43.
48. Yamane, M. A.; Williams, A. C.; Barry, B. W. *J. Pharm. Pharmacol.* **1995**, *47*, 978.
49. Jacobi, U.; Kaiser, M.; Toll, R.; Mangelsdorf, S.; Audring, H.; Otberg, N.; Sterry, W.; Lademann, J. *Skin Res. Technol.* **2007**, *13*, 19.
50. Herkenne, C.; Naik, A.; Kalia, Y. N.; Hadgraft, J.; Guy, R. H. *Pharm. Res.* **2006**, *23*, 1850.
51. Meyer, W.; Schwarz, K.; Neurand, K. T. *Curr. Probl. Dermatol.* **1978**, *7*, 39.
52. Wilkinson, S. C.; Maas, W. J. M.; Nielsen, J. B.; Greaves, L. C.; Sandt, J. J. M.; Williams, F. M. *Int. Arch. Occup. Environ. Health* **2006**, *79*, 405.
53. Rowat, A. C.; Kitson, N.; Thewalt, J. L. *Int. J. Pharm.* **2006**, *307*, 225.
54. Barone, V.; Cossi, M. *J. Phys. Chem. A* **1998**, *102*, 1995.
55. Jin, Y.; Lee, S. K.; Lee, D. W. Yonsei University, Seoul, South Korea.